A new approach for computing the steady state fluid–structure interaction response of periodic problems

Maljaars, P. J.; Kaminski, M. L.; Besten, J. H.den

DOI
10.1016/j.jfluidstructs.2018.10.002

Publication date
2019

Document Version
Accepted author manuscript

Published in
Journal of Fluids and Structures

Citation (APA)
Maljaars, P. J., Kaminski, M. L., & Besten, J. H. D. (2019). A new approach for computing the steady state fluid–structure interaction response of periodic problems. *Journal of Fluids and Structures*, *84*, 140-152. https://doi.org/10.1016/j.jfluidstructs.2018.10.002

A new approach for computing the steady state fluid-structure interaction response of periodic problems

P.J. Maljaars, M.L. Kaminski, J.H. den Besten

Delft, University of Technology, Maritime & Transport Technology Department

Abstract

A special type of fluid-structure interaction (FSI) problems are problems with periodic boundary conditions like in turbomachinery. The steady state FSI response of these problems is usually calculated with similar techniques as used for transient FSI analyses. This means that, when the fluid and structure problem are not simultaneously solved with a monolithic approach, the problem is partitioned into a fluid and structural part and that each time step coupling iterations are performed to account for strong interactions between the two sub-domains. This paper shows that a time-partitioned FSI computation can be very inefficient to compute the steady state FSI response of periodic problems. A new approach is introduced in which coupling iterations are performed on periodic level instead of per time step. The convergence behaviour can be significantly improved by implementing existing partitioned solution methods as used for time step coupling (TSC) algorithms in the time periodic coupling (TPC) framework. The new algorithm has been evaluated by comparing the convergence behaviour to TSC algorithms. It is shown that the number of fluid structure evaluations can be considerably reduced when a TPC algorithm is applied instead of a TSC. One of the most appealing advantages of the TPC approach is that the structural problem can be solved in the frequency domain resulting in a very efficient algorithm for computing steady state FSI responses.

Keywords: Fluid-structure interaction, Time periodic coupling, Partitioned solution methods, Strong coupling, quasi-Newton methods

1. Introduction

Over the past decade many papers have been published on fluid-structure interaction for different types of coupled problems. Examples of FSI problems studied in literature are for instance parachute dynamics [1, 2], flutter analysis of wings [3], airbag deployment [4], blood flow in arteries [1, 5] and hydro-elastic analysis of flexible propellers [6, 7].
Monolithic or partitioned approaches can be used to solve the coupled problems. In the monolithic approach the fluid and structure problem are simultaneously solved using a single code. In a partitioned approach the fluid and structure problem are solved in separate codes. In case of strong interaction between fluid and structure, a partitioned approach requires coupling iterations to converge to the monolithic solution, which can be computationally intensive. An important advantage of the partitioned approach is that existing codes can be used.
A straightforward partitioned solution method is the Gauss-Seidel method in which the fluid and structure problem are solved alternately and the last solution is taken as update. The convergence rate of the Gauss-Seidel method is inversely proportional with the ratio between fluid added mass and structural mass. Instability occurs when this ratio exceeds one [8]. It has been shown that the added mass of compressible flows is proportional to the time step, whereas the added mass of an incompressible flow is constant and time step size independent [8, 9] meaning that added mass instabilities in incompressible flows cannot be solved by reducing the time step size.
Several partitioned solution methods have been presented in literature for FSI problems with strong fluid added mass effects, like Aitken under-relaxation [10] and Quasi-Newton inverse least squares (QN-ILS) [11]. Where the first one belongs to the general class of stationary iterative methods and the latter one to the class of Krylov subspace methods. In combination with coupling iterations for each time step, these methods have been used in the past to converge to the solution of the fully coupled problem.
A special class of FSI problems involve periodic boundary conditions like in turbomachinery. A common approach is to solve these problems with similar approaches as used in non-periodic problems, which means with fully time step coupled (TSC) simulations [12]. An important drawback of this approach is that the transient FSI response is calculated as well and any transients in the solution procedure will adversely affect the convergence to the steady state solution.

The aim of this paper is to introduce a new approach, called the time periodic coupling (TPC) to get rid of the transient response in order to compute more efficiently the steady state response of periodic FSI problems with strong fluid added mass effects. The motivation for this work follows from our research on the hydro-elastic analysis of flexible composite propellers [13, 14]. These problems involve periodic boundary conditions and include strong fluid added mass effects [14], which require a strong coupling approach. The conceptual idea of a time periodic FSI coupling approach comes from [15] but has been applied only to a weakly coupled problem so far. The scope of this work is to introduce a TPC approach for strongly coupled FSI problems and to demonstrate the efficiency improvement for some fundamental FSI problems. It will be shown that convergence problems as appearing in TSC schemes due to strong fluid added mass effects, arise in the TPC as well. In order to stabilize a TPC scheme two partitioned solution methods used in TSC schemes, are applied in the TPC framework. The authors have limited themselves to the implementation of the Aitken under-relaxation and the QN-ILS method. The first one because it shows that a TPC approach not automatically performs better than a TSC. The later one because the QN-ILS method is the state of art in advanced under-relaxation methods in FSI calculations [16] and it shows that a TPC in combination with QN-ILS can outperform a TSC. Furthermore, with these two methods both the general class of stationary iterative methods and Krylov subspace methods have been represented. Demonstrating the performance of the TPC approach for other partitioned solution methods, which may belong to the aforementioned general classes, was considered out of the scope of this work.
The contents of this paper are organized as follows: Section 2 provides background information ib partitioned FSI, Aitken under-relaxation and the QN-ILS method. Section 2 also presents the concept of the TPC approach. Section 3 introduces some fundamental FSI problems, which have been analysed in this work. Section 4 compares TSC and TPC solutions for the problems presented in Section 3. It is shown that both approaches converge to the exact solutions. Furthermore, the TSC and TPC algorithms have been evaluated by investigating the convergence behaviour for different settings. Section 5 contains conclusions and recommendations.

2. Partitioned solution methods

In this section the time periodic FSI coupling approach is introduced in combination with two methods to keep the coupling iterations stable. First of all, the Aitken under-relaxation which belongs to the general class of stationary iterative methods. Secondly, the QN-ILS method which belongs to the general class of Krylov subspace methods.

2.1. Fluid-structure interaction

With $\mathcal{F}$ and $\mathcal{S}$ the fluid and structure operators, a partitioned fluid-structure interaction problem can be written as,

$$\begin{aligned} \mathbf{y} &= \mathcal{F}(\mathbf{x}) \\ \mathbf{x} &= \mathcal{S}(\mathbf{y}) \end{aligned} \tag{1}$$

where $\mathbf{x}$ is the structural response of the fluid-structure interface, $\mathbf{y}$ the fluid loading on the interface. The coupled problem can be formulated as solving for $\mathbf{x}$ or $\mathbf{y}$ by satisfying,

$$\mathcal{R}_{\mathbf{x}}(\mathbf{x}) = \mathcal{S} \circ F(\mathbf{x}) - \mathbf{x} = \mathbf{0} \tag{2}$$

$$\mathcal{R}_{\mathbf{y}}(\mathbf{y}) = \mathcal{F} \circ S(\mathbf{y}) - \mathbf{y} = \mathbf{0} \tag{3}$$

where $\mathcal{R}_{\mathbf{x}}$ and $\mathcal{R}_{\mathbf{y}}$ are the interface residual functions for structural response and fluid loading respectively. It is more convenient to solve for $\mathcal{R}_{\mathbf{y}}$ as will be explained in Section 2.5. When the Jacobian $\frac{\partial \mathcal{R}}{\partial \mathbf{y}}$ is known, Newton's method can be applied to find the roots of Eq. 3,

$$\mathbf{y}^{k+1} = \mathbf{y}^k - \left(\frac{\partial \mathcal{R}}{\partial \mathbf{y}}\right)^{-1} \mathbf{r}_y^k \tag{4}$$

where k denotes the coupling iteration number and the residual, $\mathbf{r}_y^k$, is defined as,

$$\mathbf{r}_{\mathbf{y}}^k = \mathcal{R}_{\mathbf{y}}\left(\mathbf{y}^k\right). \tag{5}$$

2.2. Coupling strategies for partitioned FSI problems

In case of a black-box coupling the inverse Jacobian is usually not known and time consuming to calculate. Therefore, quasi-Newton methods with approximations of the inverse Jacobian can be employed. In case the non-linearities are relatively small a straightforward approximation of the inverse

Jacobian is $-\mathbf{I}$. This approximation is basically a block Gauss-Seidel method in which the fluid and structure subsystem are solved separately and iterations are performed to converge to the fully coupled solution. For FSI problems with strong added mass effects this approach will not converge, (see for instance [17, 18]) and other quasi-Newton methods have to be applied.

2.3. Aitken under-relaxation

A method to stabilize coupling iterations is to apply under-relaxation. The inverse Jacobian is approximated as $-\sigma\mathbf{I}$, with σ the relaxation factor in interval $(0, 1]$. An optimal relaxation factor has to be found to avoid divergence on the one hand and long computational times on the other hand. With adaptive Aitken a variable under-relaxation factor σ is computed, which reduces the number of coupling iterations compared to a fixed under-relaxation factor [10]. Two pairs of computed and predicted interface forces $(\mathbf{y}^{k-1}, \widetilde{\mathbf{y}}^{k-1})$ and $(\mathbf{y}^{k}, \widetilde{\mathbf{y}}^{k})$ are required to estimate the best prediction of the interface forces for the next coupling iteration $(\widetilde{\mathbf{y}}^{k+1})$ based on the secant method. The first step of the secant method reads,

$$\widetilde{\mathbf{y}}^{k+1} = \widetilde{\mathbf{y}}^{k} + \sigma^{k}\left(\mathbf{y}^{k} - \widetilde{\mathbf{y}}^{k}\right) \tag{6}$$

where for vector cases the following expression for σ^k has been proposed [10],

$$\sigma^{k} = -\sigma^{k-1}\frac{\mathbf{r}_{\mathbf{y}}^{k-1} \cdot \left(\mathbf{r}_{\mathbf{y}}^{k} - \mathbf{r}_{\mathbf{y}}^{k-1}\right)}{\left\|\mathbf{r}_{\mathbf{y}}^{k} - \mathbf{r}_{\mathbf{y}}^{k-1}\right\|^{2}} \tag{7}$$

Hence, with Aitken under-relaxation the relaxation parameter is adjusted based on the inner product of the residuals to control the convergence of the coupling iterations. It has been shown that the convergence behaviour of Aitken's method deteriorates as the fluid-structure mass ratio increases [8] and, therefore, more coupling iterations are required. To reduce the number of coupling iterations more efficient coupling strategies have been developed, like the QN-ILS approach described hereafter.

2.4. Quasi-Newton inverse least squares

With the QN-ILS method [11] an improved approximation of the inverse Jacobian is obtained. In the QN-ILS method the inverse Jacobian is not explicitly determined but implicitly included in the new update of the interface forces $\widetilde{\mathbf{y}}^{k+1}$. The QN-ILS method is like Aitken under-relaxation based

on known input-output pairs of Eq. 3, but in the QN-ILS method results of all previous iterates are used. The best candidate for $\widetilde{\mathbf{y}}^{k+1}$ is a vector of forces which will minimize $\mathbf{r}_{\mathbf{y}}^{k+1}$. By following [19] an approximation of the new residual vector $\mathcal{R}_{\mathbf{y}}\left(\mathbf{y}^{k+1}\right)$ is written as a linear combination of previous residual vectors,

$$\mathcal{R}_{\mathbf{y}}\left(\mathbf{y}^{k+1}\right) \approx \mathbf{r}_{\mathbf{y}}^{k} + \sum_{i=0}^{k-1} \alpha_i^k \left(\mathbf{r}_{\mathbf{y}}^{i} - \mathbf{r}_{\mathbf{y}}^{k}\right) \tag{8}$$

The coefficients α_i^k are found from a least squares minimization of the approximated residual $\mathcal{R}_{\mathbf{y}}\left(\mathbf{y}^{k+1}\right)$,

$$\boldsymbol{\alpha}^k = \arg\min_{\boldsymbol{\alpha}^k \in \mathbb{R}} ||\mathbf{r}_{\mathbf{y}}^{k} + \sum_{i=0}^{k-1} \alpha_i^k \left(\mathbf{r}_{\mathbf{y}}^{i} - \mathbf{r}_{\mathbf{y}}^{k}\right)|| \tag{9}$$

By assuming a linear relation between $\mathbf{r}_{\mathbf{y}}$ and $\mathbf{y}$, the best approximation for $\widetilde{\mathbf{y}}^{k+1}$ is the linear combination of the previous iterates of $\mathbf{y}$,

$$\widetilde{\mathbf{y}}^{k+1} = \mathbf{y}^{k} + \sum_{i=0}^{k-1} \alpha_i^k \left(\mathbf{y}^{i} - \mathbf{y}^{k}\right) \tag{10}$$

Eq. 10 shows that the approximate inverse Jacobian is implicitly included in the expression $\sum_{i=0}^{k-1} \alpha_i^k \left(\mathbf{y}^i - \mathbf{y}^k\right)$. Any linear combination of changes in fluid forces that are obtained from previous iterates are coupled implicitly. The coupling is explicit for the changes in fluid forces that cannot be written as a linear combination of previous iterates. Since the most unstable variations will directly appear in the solution process, they will be included in the approximation of the inverse Jacobian and, therefore, implicitly coupled immediately after performing QN-ILS coupling iterations [20].

2.5. Time step coupling and time periodic coupling

For calculating the steady state response of FSI problems with periodic boundary conditions TSCs are frequently applied. A typical algorithm is shown as Algorithm 1. A certain number of FSI cycles, n_{FSI}, have to be performed until the steady state solution is obtained. To initialize the FSI computation first $\widetilde{\mathbf{y}}_{1..N}^1$ have to be defined, where N is number of time steps in one period and the superscript 1 refers to the coupling iteration number. This is accomplished by first computing $\mathbf{y}_{1..N}$ from a calculation in which no

fluid-structure coupling is involved. Then, $\mathbf{y}_{1..N}$ is taken as the best candidate for $\widetilde{\mathbf{y}}^1_{1..N}$. Each time step, k coupling iterations are applied until $\|\mathbf{r}\|$ is smaller than a specified tolerance ϵ. The best candidate $\widetilde{\mathbf{y}}^{k+1}_n$ for the next coupling iteration is, for instance, calculated with Aitken under-relaxation or the QN-ILS method. Algorithms for these two methods can be found in [16].

In the TPC algorithm the periodicity in the problem has been utilized to avoid coupling iterations on time step level. An algorithm for a TPC is presented as Algorithm 2. A certain number of FSI cycles have to be performed until the FSI problem is converged. The number of FSI cycles coincides with the number of coupling iterations k. In line 13 of Algorithm 2 the best candidates $\widetilde{\mathbf{y}}^{k+1}_{1..N}$ for the interface forces at all time steps for the next FSI cycle are calculated, for instance with Aitken under-relaxation or the QN-ILS method. The TPC algorithm shows that the structural and fluid sub-problem comprises the steady state solutions for both sub-problems. For a fast convergence we propose to solve fluid and structural problem, if possible, in the frequency domain. Thus, the steady state solutions for the two sub-problems are immediately obtained and any transients in the solutions, which will slow down the convergence to the steady-state FSI solution, are not computed.

Note, that the algorithms might also start with the fluid evaluations in line 9 and line 8 of Algorithm 1 and 2, respectively. Then, line 11 of Algorithm 1 and line 13 of Algorithm 2 will change in calculating the best candidate for the structural displacements. However, also the structural velocity and acceleration are coupled to the fluid and, therefore, $\widetilde{\dot{\mathbf{x}}}^{k+1}$ and $\widetilde{\ddot{\mathbf{x}}}^{k+1}$ have to be approximated as well. That would require an additional calculation step, therefore, Algorithms 1 and 2 have been followed for the computations in this work.

Algorithm 1 Algorithm for a time step coupling

$n_{FSI} = 0$
Define $\widetilde{\mathbf{y}}_{1..N}^{1}$
while FSI problem not converged **do**
    $n_{FSI} = n_{FSI} + 1$
    for $n = 1 : N$ **do** ▷ *With N the number of time steps in a period*
        $k = 0$
        while $\left\|\mathbf{r}_n^{k-1}\right\| > \epsilon$ **do**
            $k = k + 1$
            $\mathbf{y}_n^k = \mathcal{F} \circ \mathcal{S}\left(\widetilde{\mathbf{y}}_n^k\right)$
            $\mathbf{r}_n^k = \mathbf{y}_n^k - \widetilde{\mathbf{y}}_n^k$
            Calculate $\widetilde{\mathbf{y}}_n^{k+1}$
        end while
    end for
end while

Algorithm 2 Algorithm for a time periodic coupling

$n_{FSI} = 0$ $n_s = 0$ $n_f = 0$
$k = 0$
Define $\widetilde{\mathbf{y}}_{1..N}^{1}$
while FSI problem not converged **do**
    $n_{FSI} = n_{FSI} + 1$
    $k = n_{FSI}$
    for $n = 1 : N$ **do** ▷ *Calculate steady state solution for* $\mathbf{x}_{1..N}^k$
        $\mathbf{x}_n^k = \mathcal{S}\left(\widetilde{\mathbf{y}}_n^k\right)$
    end for
    for $n = 1 : N$ **do** ▷ *Calculate steady state solution for* $\mathbf{y}_{1..N}^k$
        $\mathbf{y}_n^k = \mathcal{F}\left(\mathbf{x}_n^k\right)$
    end for
    Calculate $\widetilde{\mathbf{y}}_{1..N}^{k+1}$
end while

3. Problem description

This section will describe the problems which will be solved. First a two-degree of freedom (DoF) model for pitching and plunging motions of a prismatic wing in a fluid will be presented. The FSI response of this problem will be solved with a TSC and TPC approach in which a black-box fluid solver is used. Then, a 1-DoF model for the same wing but for pitching motions only will be presented. This model has been used in another study for comparison of fluid-structure interaction algorithms [21] and will be used in this work to verify the TSC and TPC approach. Finally, this section will present a 1-DoF model, again for the same wing but for plunging motions only. This model will be used for a comparative study between the TSC and TPC approach. The problem involves strong fluid-added mass effects which are known to introduce numerical difficulties, making it a useful problem for demonstrating the benefits of the TPC approach.

3.1. 2-DoF model for pitching and plunging wing motions

The problem of interest is the motion of a prismatic wing with a span, s, of 20 m, chord, c, of 1 m and a NACA 0009 cross section profile in an incompressible flow at zero angle of attack and an incoming flow velocity, v_x, of 3 m/s (Figure 1). The wing is connected with springs to a structure and can rotate around the mid-chord point and move in vertical direction. The wing is subjected to an external harmonic force and moment,

$$\mathbf{f}_0 = \begin{Bmatrix} f_z \\ m_\theta \end{Bmatrix} = \begin{Bmatrix} F_z \\ M_\theta \end{Bmatrix} cos(\omega t) \tag{11}$$

where F_z and M_0 are the force and moment amplitudes, 400,000 N and 10,000 Nm, respectively. ω is the radial frequency in rad/s and unless specified otherwise the excitation frequency is 4π rad/s. Due to the external loads the wing oscillates in pitching and plunging motion. The equation of motion with respect to the centre of motion (COM) for this problem reads,

$$\mathbf{M}\ddot{\mathbf{u}} + \mathbf{C}\dot{\mathbf{u}} + \mathbf{K}\mathbf{u} = \mathbf{f}_0 + \mathbf{f}_h(\mathbf{u}, \dot{\mathbf{u}}, \ddot{\mathbf{u}}) \tag{12}$$

where the vector $\mathbf{u}$ contains the vertical displacement, z, and rotation of the wing, θ, $\mathbf{f}_h$ is the vector with hydrodynamic loads due to the wing structural response. $\mathbf{M}$, $\mathbf{K}$ and $\mathbf{C}$ denote the mass, stiffness and damping matrices. The mass of the wing is 1,000 kg, the rotational inertia is 100 kgm^2. The

centre of gravity (COG) is 0.05 m in front of the COM. Hence, the mass matrix is given by,

$$\mathbf{M} = \begin{bmatrix} 1,000 & 50 \\ 50 & 100 \end{bmatrix} \tag{13}$$

The extensional spring stiffness is 7,500,000 N/m and the stiffness of the torsional spring is 375,000 Nm/rad. Hence, the stiffness matrix is given by,

$$\mathbf{K} = \begin{bmatrix} 7,500,000 & 0 \\ 0 & 375,000 \end{bmatrix} \tag{14}$$

Unless specified otherwise, 5% critical damping, ζ, of the individual springs has been used as default for the damping terms in the structural damping matrix. The reason for this high value will be explained in Section 4.2.4. Hence, the damping matrix is given by,

$$\mathbf{C} = \begin{bmatrix} 8,660 & 0 \\ 0 & 612 \end{bmatrix} \tag{15}$$

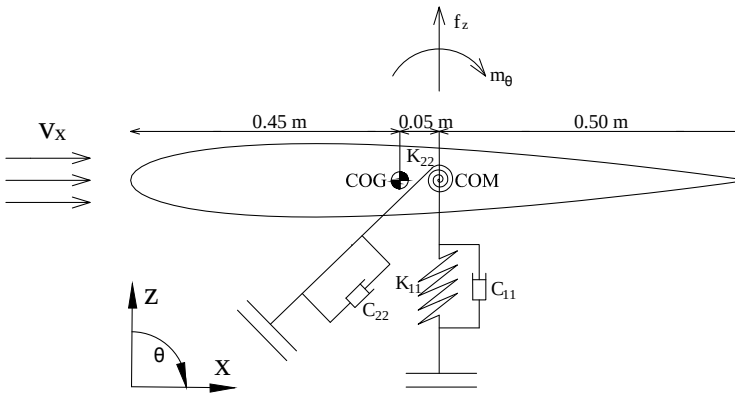

Figure 1: A two-degree of freedom model for the pitching and plunging motions of a prismatic wing.

3.2. 1-DoF model for pitching wing motions

To verify the correctness of the TSC and TPC partitioned approaches, calculations have been performed for the specific case of pitching motions only. For that case the 2-DoF model reduces to,

$$M_{22}\ddot{\theta} + C_{22}\dot{\theta} + K_{22}\theta = m_0 - m_h(\theta, \dot{\theta}, \ddot{\theta}) \tag{16}$$

with θ the pitch angle. For this typical problem approximation formulas for m_h, subdivided in fluid added mass, fluid damping and fluid stiffness loads, have been approximated based on incompressible viscous Reynolds-averaged Navier-Stokes (RANS) computations [22]. The approximation formulas for fluid added mass, m_f, fluid damping, c_f and fluid stiffness, k_f read,

$$\begin{aligned}
m_h &= -m_f\ddot{\theta} - c_f\dot{\theta} - k_f\theta \\
m_f &= \frac{\pi}{128}\rho c^4 s \\
c_f &= \begin{cases} 0.105k^{-0.4}\rho v_x c^3 s & \text{for k}\leq 4, \\ 0.010k^{0.6}\rho v_x c^3 s & \text{for k}\geq 12, \end{cases} \\
k_f &= \begin{cases} (0.090k - 0.80)\,\rho v_x^2 c^2 s & \text{for k}\leq 4, \\ (0.065k - 0.90)\,\rho v_x^2 c^2 s & \text{for k}\geq 12, \end{cases}
\end{aligned} \tag{17}$$

where k is the reduced frequency that describes the unsteadiness of the flow,

$$k = \frac{\omega c}{2v_x} \tag{18}$$

With these approximations the equation for the pitching motion is,

$$M_{22}\ddot{\theta} + C_{22}\dot{\theta} + K_{22}\theta = m_0 - m_f\ddot{\theta} - c_f\dot{\theta} - k_f\theta. \tag{19}$$

3.3. 1-DoF model for plunging wing motions

A comparison of the TSC and TPC approach have been performed for the specific case of plunging motions only. In that case the 2-DoF model reduces to,

$$M_{11}\ddot{z} + C_{11}\dot{z} + K_{11}z = f_z - f_h(\dot{z}, \ddot{z}) \tag{20}$$

with z the vertical plunge displacement and f_h the hydrodynamic loads due to the vertical plunge motion only. For high reduced frequencies the fluid forces due to the plunging of the wing are dominated by the non-circulatory lift [14, 23]. The non-circulatory lift part can be expressed as a fluid-added mass, m_a, times the acceleration [14, 23], meaning Eq. 20 can be converted into,

$$M_{11}\ddot{z} + C_{11}\dot{z} + K_{11}z = f_z - m_a\ddot{z} \tag{21}$$

In general Eq. 21 can be written as,

$$(M_{11} + \lambda m_a)\,\ddot{z} + C_{11}\dot{z} + K_{11}z = f_z + (\lambda - 1)\,m_a\ddot{z} \tag{22}$$

where λ is called the fluid added mass fraction which controls the amount of fluid added mass in left- and right-hand-side of the equation. For λ a value from the interval $[0, 1]$ has to be taken, where for $\lambda = 0$ the problem is fully partitioned and for $\lambda = 1$ the monolithic solution is obtained.
The added mass of the wing has been calculated with the method described in [7, 14] and is approximately 16,000 kg. The advantage of this 1-DoF problem is that the exact Jacobian of the residual function is irrespective of the excitation frequency and can be easily derived. The Jacobian of the residual function is the derivative of the residual function $\mathcal{R}_y$ with respect to the fluid loads on the interface, for the 1-DoF case denoted by y. For the plunging problem for any time step n, Eq. 3 can be written as,

$$\mathcal{R}_{y_n} = f_{z_n} - m_a \ddot{z}_n - y_n \tag{23}$$

A direct relation between $\ddot{z}_n$ and y_n exists and follows from the time integration scheme. In the TSC coupling the average constant acceleration Newmark scheme has been used. This scheme is unconditionally stable without numerical damping. This yields the following relation between $\ddot{z}_n$ and y_n,

$$\ddot{z}_n = S^{-1} \left(y_n - C_{11} \dot{z}_n^* - K_{11} z_n^* \right) \tag{24}$$

where $\dot{z}_n^*$ and z_n^* are the velocity and displacement estimates at timestep n, respectively. S denotes the Newmark time stepping matrix, which for the 1-DoF problem is equal to,

$$S = M_{11} + \gamma \Delta t C_{11} + \beta \Delta t^2 K_{11} \tag{25}$$

with $\gamma = 1/2$ and $\beta = 1/4$ for the Newmark average constant acceleration scheme. Then, the derivative of the residual function to y_n is equal to,

$$\frac{\partial \mathcal{R}_{y_n}}{\partial y_n} = -\left(\frac{m_a}{S} + 1 \right) \tag{26}$$

4. Fluid-structure interaction analyses

This section will present the results of the FSI calculations. The different analyses have been structured as follows: first of all, results obtained with the TSC and TPC approach for the 1-DoF pitching problem will be shown together with the analytical solutions in order to verify the correctness of the coupling approaches. Secondly, a comparison of the convergence behaviour

of the TSC and TPC approach will be presented from the results obtained for the 1-DoF plunging problem. This section concludes with a TSC and TPC calculation of the 2-DoF problem in order to show the efficiency improvement of the new approach for the more common case that fluid forces are computed with a black-box fluid solver.

4.1. Verification of TSC and TPC approach for 1-DoF pitching problem

In order to verify the TSC and TPC approach, partitioned solutions for the 1-DoF pitching problem have been compared to the exact monolithic solutions. The monolithic solutions are obtained by moving the fluid forces from the right-hand-side of Eq. 19 to left-hand-side and then the exact solution for θ can be computed. The partitioned solutions are obtained by keeping the fluid forces in the right-hand-side as unknowns and iterations are required to converge to the monolithic solution. Fig. 2 shows the exact solution, the TSC solution and the TPC solution for the oscillation frequencies $\{4\pi, 7\pi, 10\pi\}$ rad/s, i.e. stiffness, damping and mass dominated response regimes. For all cases the TSC and TPC procedure converges to the exact solution. The figures show also the number of FSI cycles, n_{FSI}, required for convergence. For convergence the criterion that the root mean square of the relative difference in fluid forces between subsequent FSI cycles should be smaller than 0.1% has been used. The results show that for all the cases the number of FSI cycles is significantly smaller when TPC has been used. In the next subsection the benefits of the TPC coupling will be further explored for the 1-DoF plunging problem.

4.2. Comparison of TSC and TPC approach for the 1-DoF plunging problem

The benefits of the TPC coupling are demonstrated using the 1-DoF plunging problem by comparing the performance of the TSC and TPC algorithms for different settings and using Aitken or the QN-ILS method for the approximation of the best candidate for the fluid interface forces. All the TSC calculations for the 1-DoF plunging problem are performed using the exact Jacobian as derived in Section 3.3. Therefore, the results obtained with the TPC algorithm are always compared to the most efficient TSC algorithm, since for a TSC framework the fastest convergence of the FSI problem is obtained with the exact inverse Jacobian.

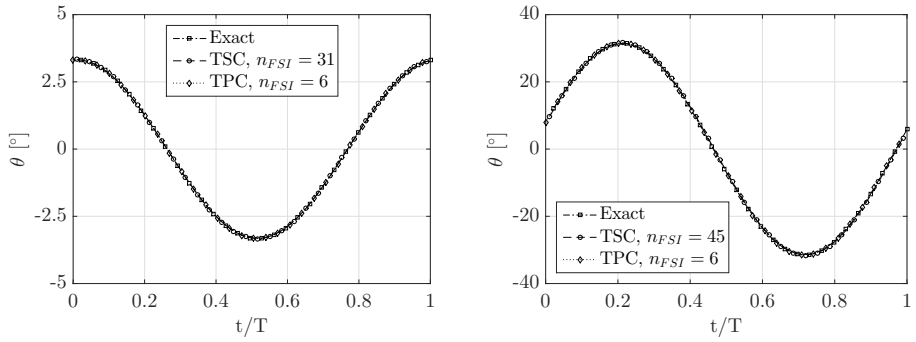

(a) $\omega = 4\pi$

(b) $\omega = 7\pi$

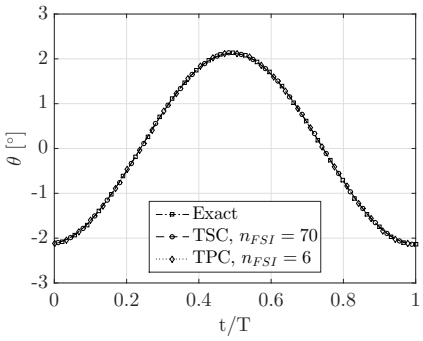

(c) $\omega = 10\pi$

Figure 2: Exact, TSC and TPC solution for θ as a function of the normalized time, t/T, $T = 2\pi/\omega$, for the 1-DoF pitching problem.

4.2.1. Time step and Aitken time periodic solution for different fluid added mass fractions

The convergence of the TSC algorithm with the exact (inverse) Jacobian of the residual function and the TPC algorithm with Aitken under-relaxation will be compared for the 1-DoF plunging problem for different fluid added mass fractions. Both algorithms have to run through a number of FSI cycles until a steady state FSI response is obtained. After each FSI cycle the error, ψ, is calculated from:

$$\psi_n = \frac{y_n^k - \widetilde{y}_n^k}{y_n^k} \qquad n = 1 \dots N \tag{27}$$

$$\psi = rms \begin{Bmatrix} \psi_1 \\ \vdots \\ \psi_N \end{Bmatrix}$$

The error as a function of the number of FSI cycles is depicted in Figure 3 for various values of λ. For $\lambda = 1$ a monolithic problem is solved and both algorithms are directly converged, since in that case y includes only the non-oscillating wing forces, f_z. For smaller fluid added mass fractions the TSC requires only two coupling iterations per time step; after the first sub-iteration only one corrector step is needed since the exact (inverse) Jacobian of the residual function is known and the residual function, $\mathcal{R}_y$, is linear in the accelerations. Hence, the number of structure and fluid evaluations is $2n_{FSI}N$ in case of the TSC, while this is $n_{FSI}N$ for the TPC. The factor 2 comes from the number of coupling iterations for each time step, which is the minimum number of coupling iterations for the TSC approach.
The results show that the convergence of the TSC is hardly influenced by the fluid added mass fraction. The opposite is the case for the Aitken TPC. When λ becomes too small, the Aitken TPC does not converge. While depending on λ a faster convergence could be obtained with the TPC compared to the TSC.

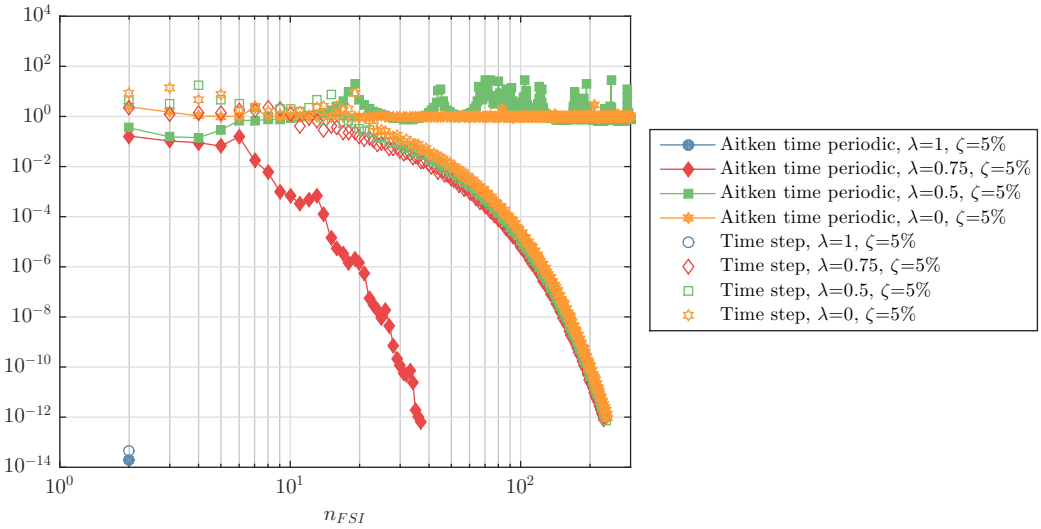

Figure 3: Convergence behaviour of the time step and Aitken time periodic coupling for the 1-DoF plunging problem for different fluid added mass fractions.

4.2.2. Time step and QN-ILS time periodic solution for different fluid added mass fractions

For the TPC a faster convergence rate can be obtained when a better approximation of the inverse Jacobian of the residual function is included. For that reason the QN-ILS approach has been implemented in the TPC. Results obtained with the TSC and QN-ILS TPC for the 1-DoF plunging problem for different fluid added mass fractions are depicted in Figure 4. This figure shows that the QN-ILS TPC, in contrast to the Aitken TPC, converges for any λ. For subsequent coupling iterations instabilities in the solution process are included in the approximation of the inverse Jacobian of the residual function and, therefore, implicitly coupled directly after performing QN-ILS coupling iterations [20], keeping the solution process stable even for strong instabilities due to fluid added mass effects. Furthermore, it can be concluded that the number of FSI cycles needed for convergence is smaller for the QN-ILS TPC than for the TSC for any λ. The results show also that the convergence behaviour is more or less independent of λ for the TSC. This is the case for the TPC as well, up to $\psi = 10^{-6}$. For a further convergence the calculation with $\lambda = 0$ requires more FSI cycles. In summary, it can be concluded that the QN-ILS approach stabilizes the solution process of the TPC even for strong fluid added mass effects and fewer FSI cycles are

required for convergence than with a TSC algorithm.

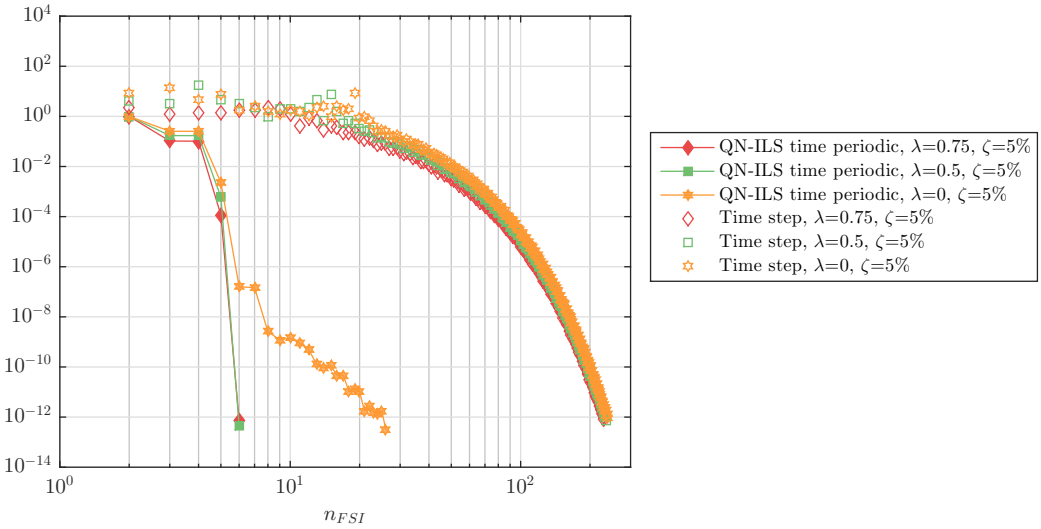

Figure 4: Convergence behaviour of the time step and QN-ILS time periodic coupling for the 1-DoF plunging problem for different fluid added mass fractions.

4.2.3. Time step and QN-ILS time periodic solution for different damping ratios

For periodic FSI problems solved in the time domain the amount of damping in the system determines the number of FSI cycles required to obtain the steady state solution. Therefore, damping has an important influence on the convergence behaviour. In order to damp the transients in the response rapidly, artificial damping could be included, but that will also alter the steady state solution. Figure 5 shows the influence of damping on the convergence of the TSC with the exact Jacobian of the residual function for the 1-DoF plunging problem. When the damping becomes too small the solution will hardly converge. The number of FSI cycles is inversely proportional to the damping ratio.

In case of the TPC, steady state solutions for the fluid and structural problem are sequentially calculated for each FSI cycle and the structural problem has been solved in the frequency domain. In that way the steady state structural solution for each FSI cycle is immediately obtained and any transients which will adversely affect the convergence to the steady state FSI solution are not computed. Figure 5 shows also the convergence of the QN-ILS TPC for different damping ratios. It can be concluded that fast damping independent convergence is obtained with the QN-ILS TPC coupling and adopting a frequency domain approach. Figure 5 explains also why the default damping value is equal to the high value of 5% of the critical damping. This value has been chosen in order to avoid biasing of the results in favour of the new coupling approach. Since for low damping the TPC approach will outperform the TSC even more.

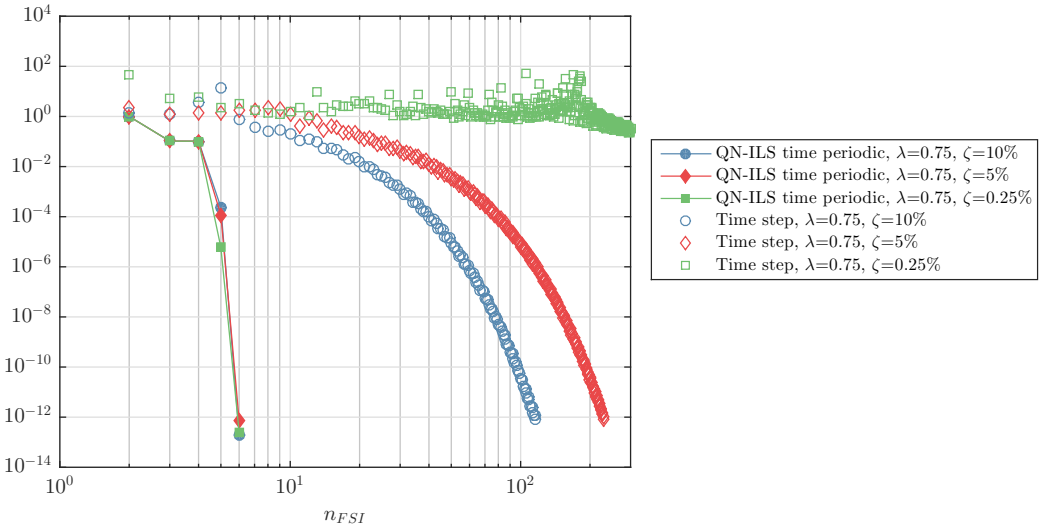

Figure 5: Convergence behaviour of the time step and QN-ILS time periodic coupling for the 1-DoF plunging problem for different fluid added mass fractions.

4.2.4. Time step and QN-ILS time periodic solution for different oscillation frequencies

The convergence of the TSC algorithm with the exact (inverse) Jacobian of the residual function and the QN-ILS TPC algorithm will be compared for the 1-DoF plunging problem for the oscillation frequencies $\{4\pi, 7\pi, 10\pi\}$ rad/s. Since, the wet natural frequency (i.e. the natural frequency including the fluid added mass contribution) is 21 rad/s, the three oscillation frequencies cover stiffness, damping and mass dominated response regimes.
Figure 6 shows the convergence behaviour of the two algorithms. For any case the convergence rate of the QN-ILS TPC algorithm is much faster than for the TSC algorithm. Up to $\psi = 10^{-6}$ the various TPC calculations converge similarly, for further convergence the number of FSI cycles strongly depends on ω. Over the whole range of errors a frequency dependency can be seen for the TSC approach. The slowest convergence is obtained for $\omega = 10\pi$, which is the case with the mass dominated response.

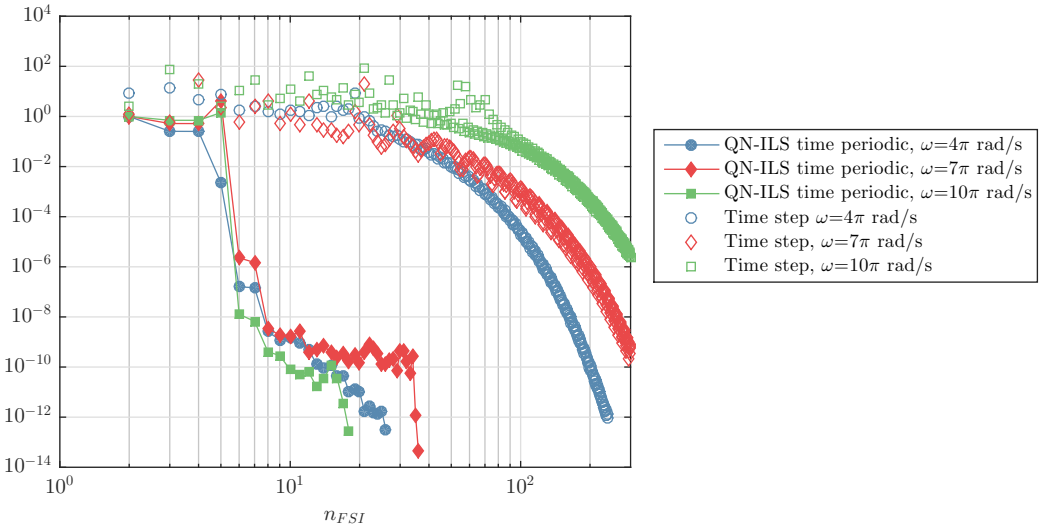

Figure 6: Convergence behaviour of the time step and QN-ILS time periodic solution for the 1-DoF problem for different oscillation frequencies.

4.3. Aitken time step and QN-ILS time periodic solution for the 2-DoF problem

In this subsection the convergence behaviour of the TSC and TPC approach will be compared for the 2-DoF problem. In the TPC calculation the structural problem has been solved in the frequency domain, and the QN-ILS method has been used to stabilize the FSI analysis. The fluid forces have been computed with the potential flow solver PROCAL [24, 25], in order to show the efficiency improvement of the new approach for the more common case that fluid forces are computed with a black-box fluid solver. In the TSC calculation Aitken under-relaxation has been used for stabilisation. The fluid forces in the TSC calculation have been obtained from the approximations for the loads as given in Eq. 17 and Eq. 21. In that way the TPC calculation has been compared to the fastest TSC calculation. Figure 7 shows the convergence of the TSC and TPC calculation, for $\omega = 4\pi$. The error has been determined with Eq. 27 by separately calculating ψ for every degree of freedom and taking the maximum of both errors.

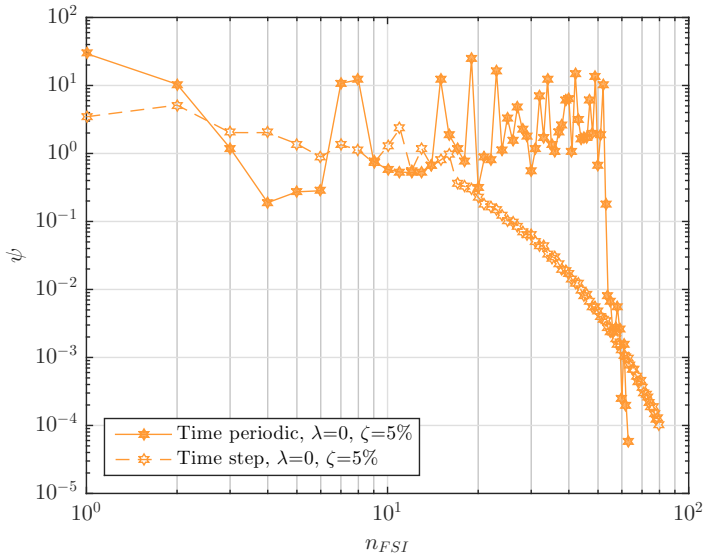

Figure 7: Convergence behaviour of the Aitken time step and QN-ILS time periodic coupling for the 2-DoF problem, $\omega = 4\pi$.

The number of FSI cycles to reduce ψ to 10^{-4} is 63 for the TPC calculation and for the TSC calculation slightly more: 75 cycles. However, as explained before, in the most optimal case the TSC calculation requires only two structure and fluid evaluations per time step, whereas for the TPC coupling this is one. In the present TSC calculation on average eight structure and fluid evaluations per time step were required, since for this two degrees of freedom problem the exact inverse Jacobian cannot be derived and is approximated with Aitken's method. Hence, it can be concluded that also for this 2-DoF case the TPC approach significantly reduces the computational demand to obtain the steady state FSI solution.
Figure 8 shows the converged solution calculated with the TPC and the black box fluid solver and the solution as obtained from the TSC calculation in which the approximations for the fluid loads have been used. The plunging response as obtained with both approaches are reasonably similar. Larger differences can be seen for the pitching response. These differences can be attributed to the following reasons. First of all, the hydrodynamic loads as obtained with the potential flow solver PROCAL will differ from the approximated loads from RANS calculations as investigated in [21]. Secondly, in the approximation formulas as used in the TSC calculation a constant

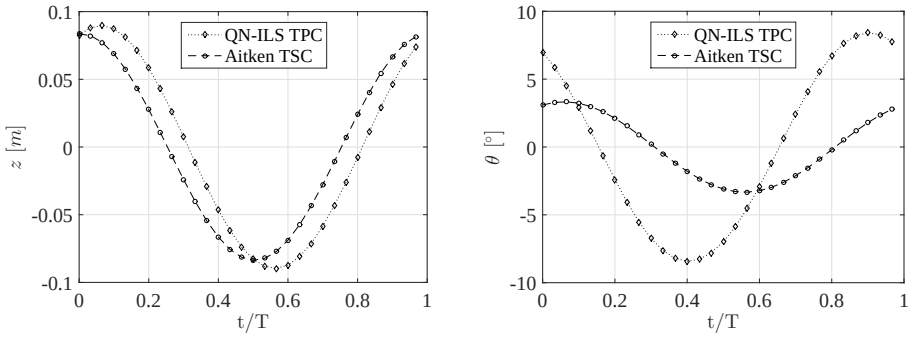

Figure 8: Aitken time step and QN-ILS time periodic solution for z and θ as a function of the normalized timed, t/T, for the 2-DoF problem, $\omega = 4\pi$.

fluid added rotation inertia has been assumed. Depending on the reduced frequency this might be wrong, since for plunging motions it has been shown that a constant added mass is only valid for sufficiently low or high reduced frequencies [14]. The most important reason is that in the TPC calculation with PROCAL the fluid forces create a coupling between plunging and pitching response. This is not present in the TSC calculation. That can be concluded from the results presented in Figures 9 and 10. These figures show results obtained with the two approaches for the 1-DoF plunging and pitching problem. That means the differences between the TPC and TSC solution can be only attributed to the first two aforementioned sources. Hence, it can be concluded that the big differences in the right graph of Figure 8 is mainly due to coupling between plunging and pitching response which is present in the TPC but not in the TSC calculation.

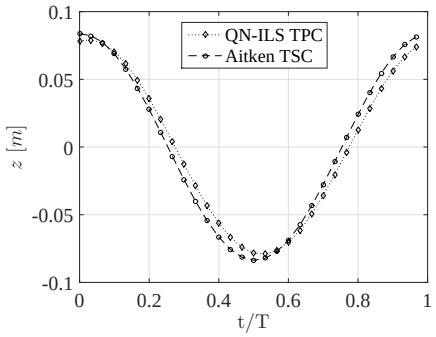

Figure 9: Aitken time step and QN-ILS time periodic solution as a function of the normalized timed, t/T, for the 1-DoF plunging problem, $\omega = 4\pi$.

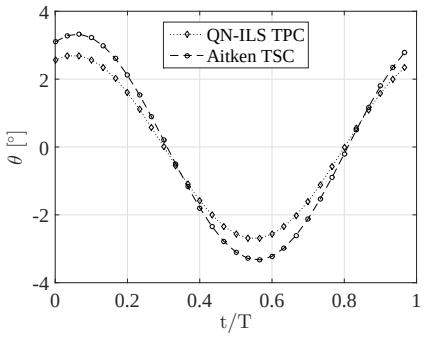

Figure 10: Aitken time step and QN-ILS time periodic solution as a function of the normalized timed, t/T, for the 1-DoF pitching problem, $\omega = 4\pi$.

5. Conclusions and recommendations

A new approach has been presented for solving more efficiently the FSI response of problems with periodic boundary conditions like in turbomachinery. It has been shown that time step coupled (TSC) simulations arduously converge to the steady state solution due to transients in the response. To get rid of the transient response the new approach is based on coupling the fluid and structural problem on a periodic level rather than per time step. In this time periodic coupling (TPC) the fluid and structural sub-problem can be solved in the frequency domain resulting in a very efficient algorithm for computing steady state FSI responses. To keep the iterative solution process stable, existing partitioned solution methods, like Aitken under-relaxation and Quasi-Newton inverse least squares (QN-ILS) have been used.
The TPC approach has been demonstrated for difficult FSI problems due to strong fluid added mass effects. The convergence rate of the TPC has been compared to a TSC approach. The results show that depending on the ratio between mass in the left- and right-hand-side of the equation of motion and damping in the system, the TPC converges much faster than a TSC. When the amount of fluid added mass in the right-hand-side of the equation of motion became too large, the Aitken TPC did not converge at all. The QN-ILS TPC converged for any case. This work shows that the computational demand to compute the steady state FSI response of periodic problems can be significantly reduced with a TPC approach.
This work has been limited to 1-DoF and 2-DoF problems. Therefore, for

future work it is recommended to analyse more extensive cases as well, preferably FSI problems comprising both potential flow and viscous flow calculations. The authors have already implemented the QN-ILS TPC approach for the more extensive problem of the hydro-elastic analysis of flexible marine propellers. This will be presented in a future publication. In this work the TPC approach have been presented only in combination with Aitken underrelaxation and the QN-ILS method. In future work the performance of the TPC approach with other partitioned solution methods should be investigated as well.

6. Acknowledgements

The authors gratefully acknowledge the Defence Materiel Organisation, Maritime Research Institute Netherlands, Wärtsilä Netherlands B.V., Solico B.V. and Nederlands Organisatie voor Wetenschappelijk Onderzoek (NWO), domain Toegepaste en Technische Wetenschappen (TTW) (project number 13278) for their financial support. The authors would gratefully thank the Cooperative Research Ships (CRS) for making their BEM software PROCAL available for this work.

[1] Y. Bazilevs, K. Takizawa, T. Tezduyar, Computational Fluid-Structure Interaction: Methods and Applications, Wiley, 2013.

[2] K. Takizawa, D. Montes, M. Fritze, S. Mcintyre, J. Boben, T. Tezduyar, Methods for FSI modeling of spacecraft parachute dynamics and cover separation, Mathematical Models and Methods in Applied Sciences 23 (2) (2013) 307–338.

[3] F. Liu, J. Cai, Y. Zhu, H. Tsai, A. Wong, Calculation of wing flutter by a coupled fluid-structure method, Journal of Aircraft 38 (2) (2001) 334–342.

[4] T. Opstal, E. van Brummelen, A potential-flow BEM for large-displacement FSI, Technical Report 3-13. Retrieved from http://www.win.tue.nl/casa/research/casareports/2012.

[5] R. Torii, M. Oshima, T. Kobayashi, K. Takagi, T. Tezduyar, Fluid-structure interaction modeling of blood flow and cerebral aneurysm: Significance of artery and aneurysm shapes, Computer Methods in Applied Mechanics and Engineering 45-46 (2) (2009) 3613–3621.

[6] P. Maljaars, J. Dekker, Hydro-elastic analysis of flexible marine propellers, In: Maritime Technology and Engineering–Edited by Guedes Soares and Santos (2014) 705–715.

[7] Y. Young, Time-dependent hydroelastic analysis of cavitating propulsors, Journal of Fluids and Structures 23 (2007) 269–295.

[8] E. van Brummelen, Partitioned iterative solution methods for fluid-structure interaction, International Journal for Numerical Methods in Fluids 65 (1-3) (2011) 3–27.

[9] E. van Brummelen, Added mass effects of compressible and incompressible flows in fluid-structure interaction, Journal of Applied Mechanics 76 (2) (2009) 021206.

[10] U. Küttler, W. Wall, Fixed-point fluid-structure interaction solvers with dynamic relaxation, Computational Mechanics 43 (2008) 61–72.

[11] J. Degroote, K. Bathe, J. Vierendeels, Performance of a new partitioned procedure versus a monolithic procedure in fluid–structure interaction, Computers Structures 87 (1112) (2009) 793–801.

[12] C. Berthold, Development of a coupled fluid-structure simulation method in the frequency domain, Master's thesis, Delft University of Technology, Delft, The Netherlands (2016).

[13] P. Maljaars, L. Bronswijk, J. Windt, N. Grasso, M. Kaminski, Experimental validation of fluidstructure interaction computations of flexible composite propellers in open water conditions using BEM-FEM and RANS-FEM methods, Journal of Marine Science and Engineering 6 (2).

[14] P. Maljaars, M. Kaminski, J. den Besten, Boundary element modelling aspects for the hydro-elastic analysis of flexible marine propellers, Journal of Marine Science and Engineering 6 (2).

[15] B. Beulen, M. Rutten, F. vandeVosse, A time-periodic approach for fluid-structure interaction in distensible vessels, Journal of Fluids and Structures 25 (5) (2009) 954–966.

[16] J. Degroote, R. Haelterman, S. Annerel, P. Bruggeman, J. Vierendeels, Performance of partitioned procedures in fluid–structure interaction, Computers Structures 88 (78) (2010) 446–457.

[17] P. Causin, J. Gerbeau, F. Nobile, Added-mass effect in the design of partitioned algorithms for fluid-structure problems, Computer Methods in Applied Mechanics and Engineering 194 (4244) (2005) 4506–4527.

[18] C. Förster, W. Wall, E. Ramm, The artificial added mass effect in sequential staggered fluid–structure interaction algorithms, European conference on computational fluid dynamics, ECCOMAS (2006) 1–20.

[19] T. Scholcz, Multi-fidelity methods for fluid-structure interaction and uncertainty quantification, Ph.D. thesis, Delft University of Technology, Delft, The Netherlands (2015).

[20] J. Degroote, P. Bruggeman, R. Haelterman, J. Vierendeels, Stability of a coupling technique for partitioned solvers in FSI applications, Computers Structures 86 (2324) (2008) 2224–2234.

[21] Y. Young, E. Chae, D. Akcabay, Hybrid algorithm for modeling of fluid-structure interaction in incompressible, viscous flows, Acta Mechanica Sinica 28 (4) (2012) 10301041.

[22] C. Münch, P. Ausoni, O. Braun, M. Farhat, F. Avellan, Fluid-structure coupling for an oscillating hydrofoil, Journal of Fluids and Structures 26 (2010) 10181033.

[23] J. Katz, A. Plotkin, Low-speed aerodynamics - 2nd ed., Cambridge University Press, 2001.

[24] G. Vaz, Modelling of sheet cavitation on hydrofoils and marine propellers using boundary element methods, Ph.D. thesis, Instituto Superior Técnico, Lisbon, Portugal (2005).

[25] G. Vaz, J. Bosschers, Modelling of three dimensional sheet cavitation on marine propellers using a boundary element method, Sixth International Symposium on Cavitation, Wageningen, The Netherlands, 2006.